The Bullet Cluster Revisited: Transport, Shocks, and Non-Equilibrium Structure

Ridwan Sakidja
Department of Physics, Astronomy and Materials Science (PAMS)
Missouri State University, Springfield, MO, USA.

Abstract

The **Bullet Cluster** is widely cited as evidence for particle dark matter because weak-lensing mass peaks are spatially offset from the X-ray–emitting gas and instead align with the collisionless galaxy component. This interpretation implicitly assumes that gravitational response must track local mass density even during a violent, dissipative merger. Here we examine a non-equilibrium interpretation within the Curvature–Transport Correspondence (CTC), in which curvature response is associated with the divergence of transport flux rather than with density alone. Using a simple and fully reproducible cartoon simulation, we show that merger-driven shocks can decouple density from coherent transport: the intracluster gas becomes dense and stalled, while collisionless components preserve ballistic motion. A nonlocal CTC diagnostic proxy defined by $\nabla^2\Psi = \nabla \cdot J$ remains aligned with the collisionless component, reproducing the observed lensing–gas offset without introducing additional collisionless matter components. These results clarify the physical assumptions underlying standard interpretations of the Bullet Cluster and emphasize the role of non-equilibrium transport during cluster mergers.

1. Introduction

The Bullet Cluster has played a central rhetorical role in the dark matter debate because it exhibits an apparent spatial separation between (i) baryonic gas traced by X-ray emission and (ii) gravitational lensing peaks typically interpreted as the dominant mass[1]. The standard claim is that the lensing peaks must represent collisionless "dark matter halos" because the gas which contains most of the baryonic mass lags behind after ram-pressure interactions and shock heating[2].

However, the cluster merger is a strongly *time-dependent, dissipative, non-equilibrium* event. In such systems, it is not generally valid to presume that any gravitational proxy must remain locally proportional to static mass density. The core question is therefore not whether gas and collisionless tracers separate (they do), but whether gravitational sourcing in such a regime must track where mass is, or may instead track where coherent transport persists.

The goal here is to articulate a clear dynamical alternative consistent with a flux-sourced curvature picture (CTC)[3]: in non-equilibrium events, density and coherent transport separate, and a curvature proxy constructed from transport divergence can remain aligned with collisionless trajectories even while the gas thermalizes.

2. Standard interpretation and its hidden equilibrium assumption

A commonly cited summary of the ΛCDM interpretation proceeds as follows. The intracluster gas is collisional and therefore undergoes shock heating, deceleration, and confinement near the interaction region. The galaxies, by contrast, are effectively collisionless on merger timescales and pass through the collision with little disruption. Because the reconstructed weak-lensing mass peaks are spatially coincident with the galaxy distribution rather than the X-ray gas, it is inferred that the dominant gravitating component must be collisionless and nonluminous[1].

This inference, however, rests on an implicit modeling assumption: that the gravitational source remains a local functional of mass density even during a strongly time-dependent, dissipative merger. In general, both Newtonian and relativistic descriptions of gravitating systems allow for contributions from momentum density, stresses, and transport processes when the system is far from equilibrium. The evidentiary strength of the Bullet Cluster therefore depends on the extent to which gravitational response is assumed to remain rigidly tied to instantaneous density, rather than to the dynamical state of transport.

3. Transport-based curvature sourcing within the CTC framing

We introduce a minimal mathematical statement of the CTC style sourcing used in this work. Let $J(x,t)$ denote an effective transport flux field, representing the flow of momentum or energy. Here J should be understood as an effective representation of momentum and energy transport encoded in the dynamical and off diagonal components of the stress energy tensor, rather than as a new fundamental field. *No modification* of the Einstein field equations is assumed; the analysis remains fully within General Relativity, provided the stress energy tensor is treated in its *original, fully dynamical form* rather than approximated by mass density alone, as emphasized in standard formulations of the theory (see, e.g., *Gravitation*[4]; *General Relativity*[5]). In relativistic language, the transport flux J corresponds schematically to momentum density and energy flux components of $T^{\mu\nu}$, whose divergence governs local stress–energy redistribution in dynamical spacetimes.

We define $S(x,t)$ as an effective scalar curvature sourcing term, representing the local geometric response associated with transport imbalance. In equilibrium or slowly evolving systems, S is often correlated with mass density, so approximations in which gravity tracks density can be adequate. In strongly non equilibrium regimes, however, coherent transport can collapse due to dissipation or shocks while density remains high.

The central assumption of the present analysis is that the relevant curvature response encoded by $S(x,t)$is more closely linked to the divergence of transport than to density alone, since the divergence ∇·J captures the local breakdown, redistribution, or redirection of coherent transport that shocks act upon directly:

$$S(x,t) \propto \nabla . J(x,t).$$

Because lensing is fundamentally nonlocal, we then introduce a nonlocal potential proxy Ψ defined by the Poisson relation

$$\nabla^2 \Psi(x,t) = \nabla . J(x,t)$$

The Poisson form is adopted solely as the minimal nonlocal operator that maps a scalar source into a spatially integrated response, reflecting the *nonlocal character* of lensing observables. We emphasize that Ψ is used here only as a diagnostic proxy for nonlocal response to transport divergence. It is not claimed that gravitational lensing is directly given by $|\Psi|$ without a fully specified relativistic theory.

The purpose of this construction is to clarify the underlying dynamical logic. When shocks destroy coherent transport in the gas while collisionless components preserve organized motion, a *transport based proxy* will *naturally remain aligned* with the galaxies even as the gas density becomes centrally enhanced[1].

This picture fits cleanly within General Relativity. Einstein's equations relate spacetime curvature *to the full stress–energy tensor $T^{\mu\nu}$, not to mass density alone.* In the stalled, shock-heated gas, the energy density term T^{00} is large, but the momentum transport terms T^{0i} are strongly reduced because shocks destroy organized motion. As a result, any curvature response tied to transport naturally weakens in this region even as the gas becomes dense. No modification of General Relativity is involved here; the analysis simply avoids collapsing $T^{\mu\nu}$to density alone. This reflects Einstein's original view that gravity responds to *the complete dynamical state of matter and energy*, not just to where mass accumulates.

4. Cartoon simulation and reproducible figure set

To make the argument transparent, we provide a minimal particle-based cartoon with two components:

- Galaxies: collisionless tracers with ballistic motion.
- Gas: collisional tracers subject to drag and strong dissipation inside a "collision zone," mimicking shock/thermalization[6,7].

We construct a coarse-grained transport (flux) field

$$J(x,t) \approx \sum_k w\,(x - x_k(t))\; v_k(t),$$

where $x_k(t)$ and $v_k(t)$ are the positions and velocities of individual particles, and $w$is a smooth weighting kernel used to deposit particle contributions onto a grid. The divergence $\nabla \cdot J$ is then computed and used as the source term for a nonlocal response potential Ψ, defined through the Poisson equation $\nabla^2\Psi = \nabla \cdot J$. The magnitude $|\Psi|$ is used solely as a diagnostic proxy for a transport-based, nonlocal response, not as a direct calculation of gravitational lensing[1]. For comparison, we also construct a ΛCDM-style "cartoon halo" by smoothing the galaxy positions with a Gaussian kernel, producing a grayscale density map. This diagnostic explicitly enforces the standard assumption that the lensing signal follows the collisionless mass distribution associated with the galaxies[1].

We show four snapshots (Figures 1–4) that follow the Bullet Cluster before, during, and after the collision. The system is a highly non-equilibrium event in which different components behave very differently. The intracluster gas is collisional and experiences strong ram pressure during core passage. This produces shocks that turn directed motion into heat, creating hot X-ray–emitting gas that slows down and collects near the interaction region. The galaxies, in contrast, interact very weakly and therefore pass through the collision almost unaffected, continuing on nearly straight paths.

The well-known separation between the X-ray gas and the gravitational lensing signal is therefore not surprising on its own. The key issue is how the lensing signal is interpreted in a rapidly evolving, non-equilibrium system. The standard interpretation assumes that gravity must always track local mass density, even during violent, dissipative events. In the Curvature–Transport Correspondence, this assumption is relaxed. Under non-equilibrium conditions, gravitational response can depend on how momentum and energy are transported, rather than on density alone. This interpretation is consistent with, and already articulated in, the Curvature Transport Correspondence paper[3], which emphasizes that the Einstein field equations couple curvature to the full stress energy tensor rather than to mass density alone in non equilibrium systems.

When merger-driven shocks disrupt the gas, its organized motion breaks down and coherent transport is lost, even as the gas becomes denser. At the same time, the collisionless galaxy component preserves

coherent, ballistic motion. In this situation, a nonlocal response constructed from the divergence of the transport field, $\nabla \cdot J$, naturally remains aligned with the galaxy trajectories. This reproduces the observed lensing–gas offset without requiring an additional collisionless matter component. Across the simulation sequence, three robust qualitative behaviors emerge:

1. *The gas slows and accumulates near the interaction region.* Directed bulk motion is reduced, and the flow becomes dominated by thermalized, disordered motion.
2. *The collisionless component remains ballistic.* Galaxies pass through the interaction region while maintaining coherent transport.
3. *A transport-based non-local proxy follows the collisionless component.* Even when gas density peaks near the interaction region, the transport-driven response remains aligned with the galaxies.

Taken together, these results show that the observed lensing–gas offset arises *naturally from a non-equilibrium separation* between mass density and coherent transport.

These outcomes reproduce the logic of the observed Bullet Cluster offset without requiring the additional interpretive step "therefore unseen collisionless mass must dominate," because the observational discriminator is not solely "collisionless vs collisional" but "coherent transport vs thermalized transport." The Bullet Cluster is an excellent discriminator against *strictly static* modified gravity models that require gravity to track baryonic density instantaneously. But it is not however, a logically decisive discriminator against dynamical, transport-sensitive alternatives. In a flux-based picture, the offset is *expected*: shocks destroy the gas's organized transport, while collisionless components retain it. The merger is therefore a test of *non-equilibrium gravitational response*, *not a unique proof of particle dark matter*.

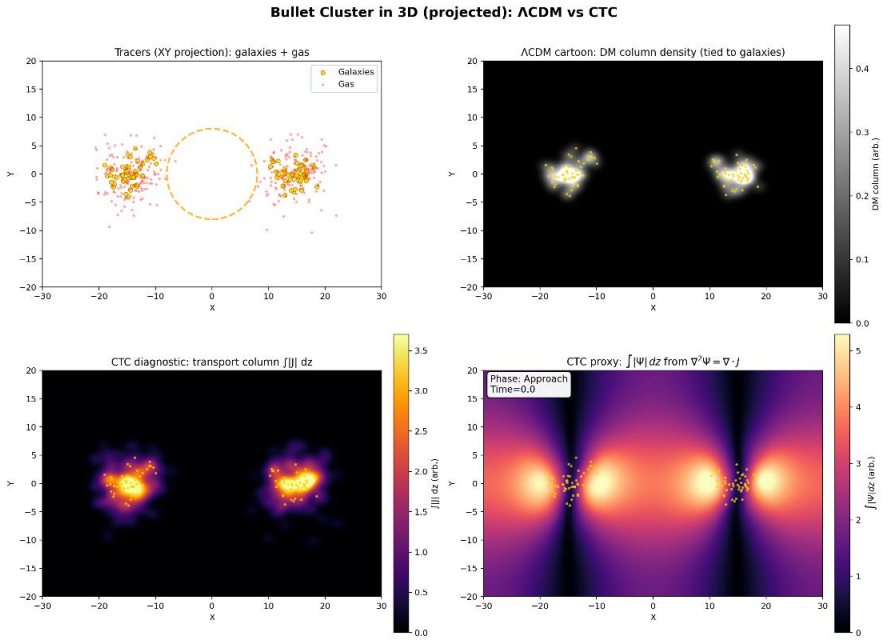

Figure 1. Pre-collision approach. Early stage of the merger prior to strong interaction. The intracluster gas (red) and galaxy populations (yellow) approach with comparable bulk velocities. In the ΛCDM cartoon (upper right), the lensing mass is assumed to follow a collisionless halo associated with the galaxies. In the CTC diagnostics (lower panels), the transport magnitude $|J|$ remains coherent across both components, and the nonlocal potential proxy $|\Psi|$, defined through $\nabla^2\Psi = \nabla \cdot J$, shows no separation between tracers at this stage.

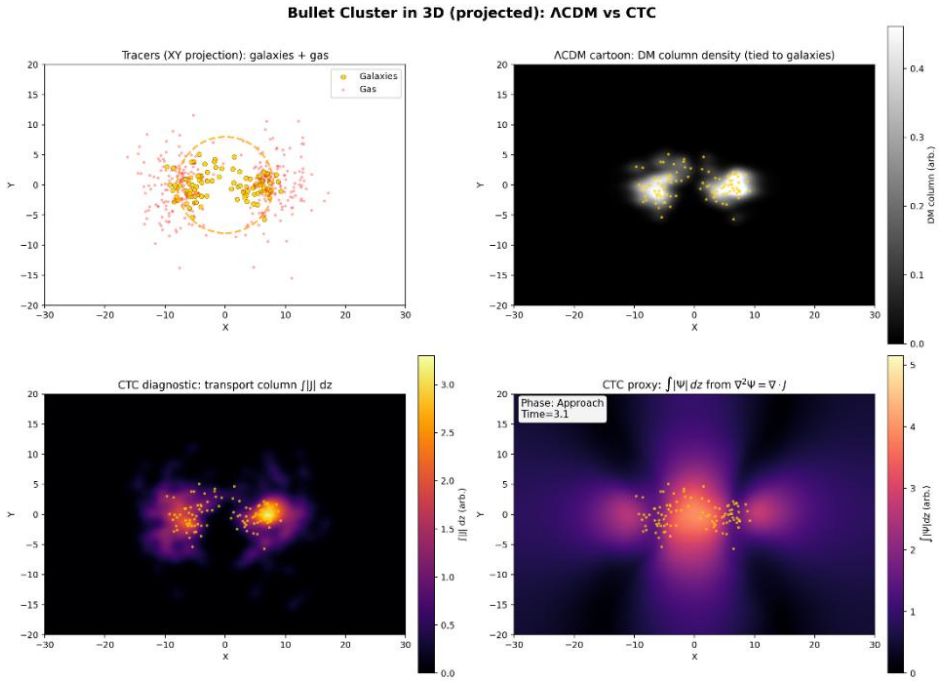

Figure 2. Onset of dissipation. As the cluster cores overlap, the collisional gas begins to experience ram-pressure interaction and shock heating, leading to deceleration and spatial broadening. The galaxies remain effectively collisionless and continue on ballistic trajectories. In the CTC panels, coherent transport in the gas is reduced within the interaction region, while transport associated with the collisionless component remains organized.

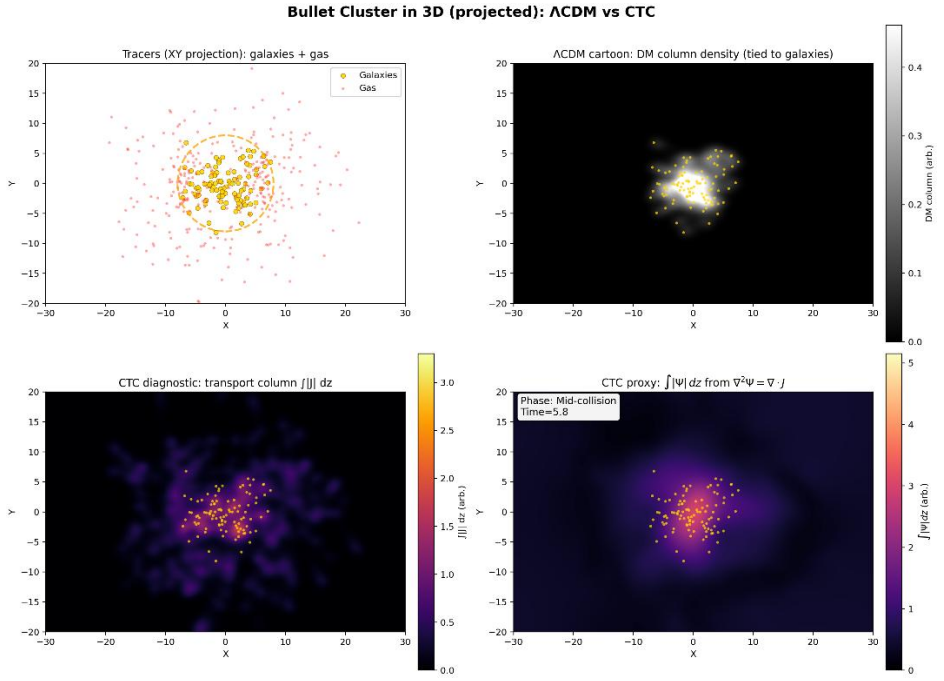

Figure 3. Mid-collision (shock-heated stall). The gas accumulates near the interaction region, reaching high density and temperature while losing directed bulk motion. Galaxies pass through the collision zone with minimal deflection. This marks the key non-equilibrium separation: *density and coherent transport decouple*. The CTC proxy $|\Psi|$, remains aligned with the collisionless transport channels despite the central concentration of gas.

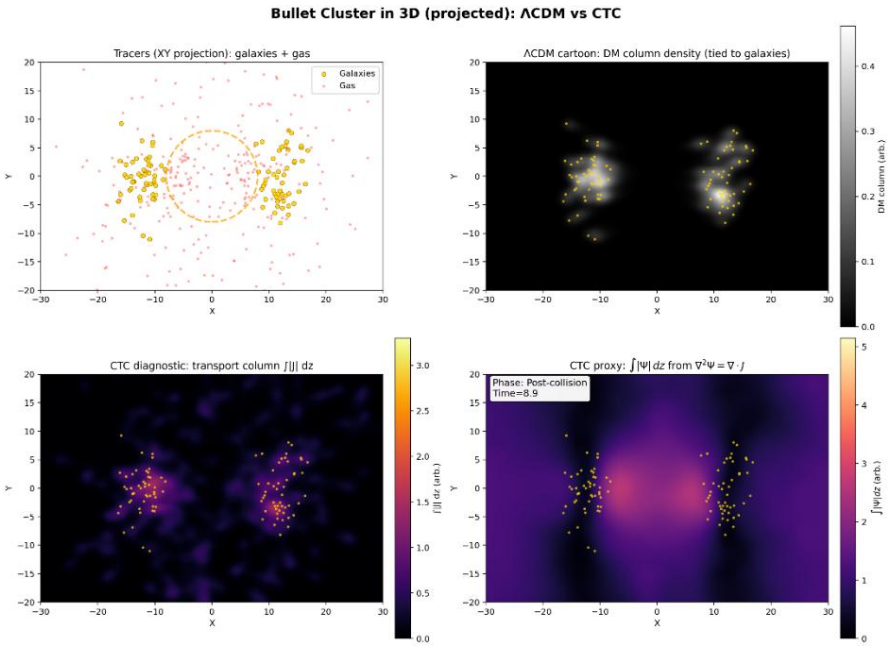

Figure 4. Post-collision offset. After core passage, the gas remains stalled near the interaction region, while the collisionless component separates into two outgoing lobes. In ΛCDM, the inferred mass distribution remains coincident with the collisionless component by assumption. In the CTC diagnostics, the nonlocal response constructed from $\nabla \cdot J$ continues to track persistent coherent transport rather than the densest baryonic material.

5. Dynamical regime diagnostics via nondimensional transport ratios

To characterize the non-equilibrium dynamics of the merger in a scale-independent way, we introduce three nondimensional diagnostic ratios constructed from the coarse-grained transport and density fields within the interaction region. These quantities are not material constants and are not assigned separately to gas and galaxies; instead, they serve as system-level indicators of the dynamical regime of the coupled gas–galaxy system during the merger. Thus, they are diagnostic measures of dynamical regime rather than invariant quantities and are introduced solely to characterize the degree of transport coherence and dissipation during the merger.

The transport coherence number

$$\Pi_J \equiv \frac{|J_{bulk}|}{\rho c_s}$$

measures how strong coherent transport is compared to the characteristic compressive response set by the gas density ρ and an effective sound speed c_s. When $\Pi_J \geq 1$, organized, ballistic transport dominates the dynamics. When $\Pi_J \ll 1$, coherent motion has largely collapsed and the flow is dominated by thermalized motion. Crossing $\Pi_J \sim 1$ therefore marks a qualitative change in the dynamical regime, not a small correction.

The second diagnostic is the dissipation (shock) number

$$D \equiv \frac{\lambda L}{v},$$

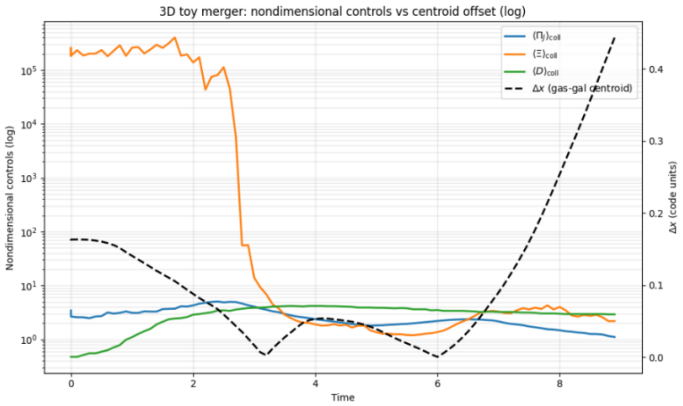

Figure 5. Time evolution of nondimensional transport diagnostics during the 3D toy merger, plotted on a logarithmic scale, together with the gas–galaxy centroid offset Δx. The transport coherence number Π_J, dissipation number D, and transport–density decoupling ratio Ξ are evaluated within the interaction region. During the collision, Ξ undergoes an order-of-magnitude collapse, indicating a breakdown of transport–density coupling under strong dissipation, while Π_J remains finite. The centroid offset grows only after this non-equilibrium transition, showing that the separation arises from transport reorganization rather than equilibrium mass segregation.

where L is the interaction length scale, v is the incoming bulk velocity, and λ is an effective dissipation rate extracted from the transport field. Small values $D \ll 1$ indicate weak dissipation, while $D \gtrsim 1$ signals strong shock dissipation and rapid loss of coherent transport.

The third diagnostic is the transport–density decoupling ratio

$$\Xi \equiv \frac{|\nabla \cdot J|}{|\nabla \rho|}.$$

This quantity measures how closely transport divergence follows density gradients. In near-equilibrium conditions, Ξ remains of order unity, meaning that transport and density vary together. In strongly shocked or non-equilibrium states, Ξ drops far below unity even as density gradients grow, indicating a breakdown of this correlation.

Overall, because these quantities are nondimensional, the physically relevant information lies in their *order-of-magnitude excursions relative to unity, rather than in their absolute numerical values*. Figure 5 shows the time evolution of Π_J, D, and Ξ on a logarithmic scale, together with the gas–galaxy centroid separation Δx. The logarithmic scale is essential: it shows that Ξ undergoes an *order-of-magnitude collapse*, not a small fluctuation around unity. This collapse occurs during the interaction phase, at the same time that the dissipation number D rises sharply, signaling strong shock activity. In contrast, Π_J remains finite, reflecting the persistence of coherent transport in the collisionless component.

Importantly, the centroid separation Δx begins to grow *after* the collapse of Ξ. This timing shows that the observed offset is linked to the breakdown and reorganization of transport during the collision, rather than to any equilibrium redistribution of mass. In this framework, the distance of each diagnostic from unity directly indicates the system's dynamical state: values near unity correspond to quasi-equilibrium behavior, while large deviations signal strongly non-equilibrium transport.

Overall, Figure 5 demonstrates that lensing–baryon–like offsets can arise naturally once shocks decouple transport from density. The key control parameter is therefore the state of transport coherence, not the instantaneous density distribution alone.

6. Shock-wave analogy from high-pressure physics

Several detailed numerical studies have demonstrated that the X-ray morphology, bow shock, and lensing–gas offsets of the Bullet Cluster can be reproduced within ΛCDM using coupled N-body and hydrodynamic simulations (e.g. Mastropietro & Burkert 2008[8]; Springel & Farrar 2007[9]). These works assume that gravitational response continues to track the collisionless mass component during the merger, while the gas responds dissipatively through shocks and ram pressure. The present study *does not* challenge the internal consistency or numerical success of such simulations. Instead, it addresses a distinct interpretive question: whether the observed offset uniquely requires an additional collisionless particle component, or whether it can arise generically from non-equilibrium transport dynamics in a shocked system.

The core physical mechanism is shock dissipation: bulk kinetic energy is converted to heat, and organized flow collapses[6,10]. In classical shock theory, a shock converts directed kinetic energy into internal energy, reducing the coherence of the bulk flux. In high-pressure hydrodynamics, shocks can create a region of high density but diminished directed transport, exactly the qualitative structure invoked here for the intracluster gas[7,10]. In the Bullet Cluster, the X-ray morphology indicates a supersonic merger with a prominent shock front, consistent with ram-pressure stripping and conversion of coherent motion to thermal energy [2]. Thus, the gas can become *dense and luminous* while losing coherent transport; meanwhile, galaxies retain ballistic transport.

The physical process highlighted by the Bullet Cluster has a close parallel in classical shock and high-pressure physics [6,10]. In compressible flows, a shock rapidly converts directed bulk motion into internal energy. As material passes through the shock, its density and temperature increase, while its organized, large-scale motion is strongly reduced. This process is described by the momentum flux across a surface,

$$\Pi = \rho u^2 + p,$$

where ρ is the mass density, u is the bulk flow speed, and p is the pressure. The term ρu^2 represents coherent transport of momentum, while p represents random, thermal motion.

Across a shock, the Rankine–Hugoniot jump conditions enforce conservation of mass and momentum,

$$\rho_1 u_1 = \rho_2 u_2, p_1 + \rho_1 u_1^2 = p_2 + \rho_2 u_2^2,$$

while the energy jump condition encodes the irreversible conversion of macroscopic kinetic energy into heat and entropy [6,10]. These relations show that although density and pressure increase downstream of the shock, the bulk velocity and hence, the directed transport term ρu^2 is accordingly reduced.

A defining feature of shocks is therefore the coexistence of high density with degraded coherent transport. Dense, hot, and luminous material can form even as organized momentum flow collapses.

The intracluster gas in the Bullet Cluster behaves in exactly this way. During core passage, merger-driven shocks and ram pressure disrupt the gas's coherent motion, producing hot X-ray–bright plasma that slows and accumulates near the interaction region. Although the gas density increases, its ability to carry organized transport is strongly reduced. In contrast, the galaxy population is effectively collisionless and continues on near-ballistic trajectories through the merger.

From a transport-based viewpoint[3], the relevant distinction is not between "visible" and "invisible" matter, but between *coherent transport and thermalized accumulation*. In the Curvature–Transport Correspondence[3], curvature response is associated with transport divergence,

$$S(\mathrm{x},\mathrm{t}) \propto \nabla . J(x,t)$$

and a nonlocal response potential Ψ is introduced through

$$\nabla^2 \Psi(\mathrm{x},\mathrm{t}) = \nabla . J(x,t)$$

In shock-heated regions where transport collapses, $\nabla . J$ can be suppressed *even when mass density is large*. Conversely, collisionless components preserve coherent transport and therefore continue to dominate the non-local response. From this perspective, the Bullet Cluster is best understood as a large-scale realization of a familiar materials-physics principle: *shocks separate density from transport,* and it is the latter that governs the system's dynamical response.

An additional indication that the Bullet Cluster represents a strongly non-equilibrium system comes from the extreme merger velocity inferred from the shock properties of the intracluster gas. Hydrodynamic modeling of the X-ray shock suggests collision velocities of order $3000 - 4700\ km/s$, [8,9,11] which lie in the far tail of the velocity distribution expected for cluster mergers in standard ΛCDM cosmology. Such high velocities are therefore *statistically rare*, and possibly inconsistent with equilibrium merger assumptions. This reinforces the interpretation that the Bullet Cluster is a dynamically extreme event, where transport, dissipation, and time-dependent effects play a dominant role. In such a regime, equilibrium intuitions about mass–density tracking are least reliable, and a transport-sensitive interpretation becomes especially relevant[12–14].

Finally, we want to emphasize that the present analysis *does not* constitute a definitive alternative to particle dark matter, nor does it claim to reproduce gravitational lensing from first principles. Rather, it provides a physically transparent proxy that isolates a key dynamical point: in a violently non-equilibrium merger, density and coherent transport need not coincide. The Bullet Cluster is therefore best understood as a stress test of equilibrium assumptions. The same shock physics invoked to interpret the system also implies conditions under which density-based sourcing becomes unreliable. In this sense, the Bullet Cluster serves not as a unique proof of dark matter, but as evidence that non-equilibrium transport effects must be carefully examined before equilibrium inferences are drawn

7. Conclusion

The Bullet Cluster offset is a real and physically significant phenomenon, but the usual "smoking gun" interpretation relies on an equilibrium assumption that gravitational response must track mass density during the merger. A transport-based interpretation, in the spirit of the Curvature–Transport Correspondence, offers a consistent non-equilibrium explanation rooted in standard shock-dissipation physics. In this picture, the collisionless component remains aligned with a transport-driven curvature proxy even when the gas becomes centrally dense and shock-heated. The next critical step is to connect flux-based sourcing to quantitative lensing observables within a fully specified framework and to test it against detailed merger reconstructions.

Acknowledgments & Data Availability

The author acknowledges support from the Matthew & Patricia Harthcock CNAS Faculty Fellowship, which enabled the pursuit of interdisciplinary research spanning astrophysics, transport physics, and computational modeling. Computational resources were provided by Missouri State University, including access to local GPU workstation infrastructure that substantially supported the simulation and analysis efforts.

This work benefited from large language model (LLM) assistance in conceptual clarification, textual refinement, and code development. The author retains full responsibility for the formulation of the study, the scientific reasoning, the validation of results, and the final interpretation presented in this paper.

All simulation scripts used in this work, including both 2D and 3D models, are publicly available at https://github.com/sakidja/CTC_related_papers/.

REFERENCES

1. Clowe, D. *et al.* A Direct Empirical Proof of the Existence of Dark Matter. *The Astrophysical Journal* **648**, L109 (2006).
2. Markevitch, M. *et al.* Direct Constraints on the Dark Matter Self-Interaction Cross Section from the Merging Galaxy Cluster 1E 0657-56. *The Astrophysical Journal* **606**, 819–824 (2004).
3. Sakidja, R. The Curvature–Transport Correspondence (CTC): From Quantum Effective Mass to Cosmological Dark Matter. (2025) doi:10.5281/zenodo.17805651.
4. Misner, C. W., Thorne, K. S., Wheeler, J. A. & Kaiser, D. I. *Gravitation*. (Princeton University Press, 2017).
5. Wald, R. M. *General Relativity*. (Chicago Univ. Pr., Chicago, USA, 1984). doi:10.7208/chicago/9780226870373.001.0001.
6. Landau, L. D. & Lifshitz, E. M. *Fluid Mechanics: Volume 6*. (Butterworth-Heinemann, 1987).
7. Toro, E. F. *Riemann Solvers and Numerical Methods for Fluid Dynamics: A Practical Introduction*. (Springer Berlin Heidelberg, 2009).
8. Mastropietro, C. & Burkert, A. Simulating the Bullet Cluster. *Monthly Notices of the Royal Astronomical Society* vol. 389 967–988 (2008).
9. Springel, V. & Farrar, G. R. The speed of the 'bullet' in the merging galaxy cluster 1E0657−56. *Monthly Notices of the Royal Astronomical Society* vol. 380 911–925 (2007).
10. Zel'dovich, Y. B. & Raizer, Y. P. *Physics of Shock Waves and High-Temperature Hydrodynamic Phenomena*. (Dover Publications, 2012).
11. Mastropietro, C. & Burkert, A. Simulating the Bullet Cluster. *Monthly Notices of the Royal Astronomical Society* **389**, 967–988 (2008).
12. Hayashi, E. & White, S. D. M. How rare is the bullet cluster? *Monthly Notices of the Royal Astronomical Society: Letters* **370**, L38–L41 (2006).
13. Lee, J. & Komatsu, E. Bullet Cluster: A Challenge to ΛCDM Cosmology. *The Astrophysical Journal* **718**, 60 (2010).
14. Thompson, R. & Nagamine, K. Pairwise velocities of dark matter haloes: a test for the Λ cold dark matter model using the bullet cluster. *Monthly Notices of the Royal Astronomical Society* **419**, 3560–3570 (2012).

Supplementary

S1. Model overview (2D and 3D models)

The simulations model the Bullet Cluster as a two-component system consisting of
(i) a collisionless component representing galaxies and
(ii) a collisional component representing the intracluster gas.

The goal is *not* to reproduce the Bullet Cluster quantitatively or to perform a full cosmological simulation. Instead, the purpose is to isolate the dynamical role of non-equilibrium transport versus density during a violent merger, and to test how these quantities separate under shock dissipation.

Galaxies are treated as ballistic tracers whose organized transport persists through the interaction. Gas particles experience dissipation, thermalization, and loss of coherent motion during core passage, mimicking the qualitative effects of shocks and ram pressure. Gravity is *not evolved dynamically.* Rather, two diagnostic constructions are compared:

1. A density-based ΛCDM cartoon, in which gravitational response is assumed to track a collisionless mass density by construction.
2. A transport-based Curvature–Transport Correspondence (CTC) diagnostic, in which a nonlocal response is tied to transport flux divergence.

Both 2D and 3D versions are implemented. The 2D model provides conceptual clarity and computational transparency, while the 3D model introduces geometric realism and line-of-sight projection consistent with lensing-style observables.

S2. Particle dynamics

Collisionless component (galaxies)

Galaxies are treated as non-interacting tracers with fixed velocities:

$$\frac{dx_i}{dt} = v_i, \frac{dv_i}{dt} = 0.$$

They preserve coherent, ballistic transport throughout the merger.

Collisional component (gas)

Gas particles obey an effective dissipative dynamics:

$$\frac{dx_i}{dt} = v_i, \frac{dv_i}{dt} = -\gamma v_i - \lambda\, \chi(x_i)\, v_i + \xi_i(t),$$

where γ represents background drag, λ enhances dissipation inside the interaction region defined by the window function $\chi(x)$, and $\xi_i(t)$ is a stochastic term modeling thermalization and isotropization.

This minimal prescription captures the essential shock behavior relevant here: *directed momentum is destroyed while mass density increases*, producing a hot, stalled gas component.

S3. Transport field and curvature proxy

A coarse-grained transport field is constructed from particle trajectories as

$$\mathrm{J}(x,t) = \sum_i m_i \; \mathrm{v}_i(t)\, W(x - x_i),$$

where W is a smooth kernel defining the coarse-graining scale.

Within the Curvature–Transport Correspondence framework, a nonlocal response potential Ψ is introduced through

$$\nabla^2 \Psi(x,t) = \nabla \cdot \mathrm{J}(x,t).$$

The quantity $|\ \Psi\ |$is used *only as a diagnostic proxy* for nonlocal response to transport divergence. It is not claimed to be a physical gravitational potential or a direct lensing observable.

S4. Dimensionality and projection

2D model
In two dimensions,

$$\nabla \cdot \mathrm{J} = \partial_x J_x + \partial_y J_y,$$

and the Poisson equation for $\Psi(x,y)$is solved using FFT-based inversion. The 2D model isolates the dynamical separation between density and transport in a planar setting.

3D model
In three dimensions,

$$\nabla \cdot \mathrm{J} = \partial_x J_x + \partial_y J_y + \partial_z J_z,$$

and the Poisson equation is solved on the full 3D grid. To construct a lensing-style diagnostic, the response is projected along the line of sight:

$$\Psi_{\mathrm{proj}}(x,y) = \int\ |\ \Psi(x,y,z)\ |\ dz.$$

This ordering i.e. first solve in 3D, then next project matches the structure of gravitational lensing observables and ensures that projection effects do not artificially generate the observed offsets.

S5. ΛCDM comparison diagnostic

For contrast, a ΛCDM-style diagnostic is constructed by assuming an explicit collisionless mass halo tied to the galaxies:

$$\rho_{\mathrm{DM}}(x) \propto \sum_{\text{galaxies}} W(x - x_i).$$

This step is *assumptive*: it enforces by construction that gravitational response tracks collisionless density, independent of transport state. The comparison therefore isolates the interpretive difference between density-tracking and transport-sensitive sourcing.